As per UGC guidelines an electronic bar code is provided to secure your paper

International Journal for Modern Trends in Science and Technology
Volume 11, Issue 06, pages 39-50.
ISSN: 2455-3778 online
Available online at: http://www.ijmtst.com/vol11issue06.html
DOI: https://doi.org/10.5281/zenodo.15576837

Advanced Power Management and Control for EV Charging Using Magnetically Linked Converters with AC-DC Load Balancing and Grid-Connected Solar, Wind, and Battery Integration

Hosuru Vinay Yadhu Vamsi[1], J. Nagaraju[2], Dr. K. Siva Kumar[3]

[1]PG Scholar, Dept. of Electrical & Electronics Engineering, Sri Venkatesa Perumal College of Engineering and Technology, Puttur, Andhra Pradesh, India
[2]Assistant Professor, Dept. of Electrical & Electronics Engineering, Sri Venkatesa Perumal College of Engineering and Technology, Puttur, Andhra Pradesh, India
[3]Professor, Dept. of Electrical & Electronics Engineering, Sri Venkatesa Perumal College of Engineering and Technology, Puttur, Andhra Pradesh, India

To Cite this Article
Hosuru Vinay Yadhu Vamsi, J. Nagaraju & Dr. K. Siva Kumar (2025). Advanced Power Management and Control for EV Charging Using Magnetically Linked Converters with AC-DC Load Balancing and Grid-Connected Solar, Wind, and Battery Integration. International Journal for Modern Trends in Science and Technology, 11(06), 39-50. https://doi.org/10.5281/zenodo.15576837

Article Info
Received: 13 May 2025; Accepted: 30 May 2025.; Published: 02 June 2025.

Copyright © The Authors ; This is an open access article distributed under the Creative Commons Attribution License, which permits unrestricted use, distribution, and reproduction in any medium, provided the original work is properly cited.

KEYWORDS

Magnetically Linked Converter, Electric Vehicle Charging, Power Management System, AC-DC Load Balancing, Grid-Connected Renewable Energy, Solar Photovoltaic (PV), Wind Energy, Battery Storage, Maximum Power Point Tracking (MPPT), Bidirectional DC-DC Converter.

ABSTRACT

This paper presents an advanced power management system for electric vehicle (EV) charging applications, integrating a magnetically linked power converter with grid-connected renewable energy sources like solar photovoltaic (PV), wind, and battery storage. The system aims to provide a reliable power supply with efficient AC and DC load balancing, supporting sustainable EV charging infrastructure. The solar PV array is connected to a DC-DC boost converter equipped with the Incremental Conductance (INC) maximum power point tracking (MPPT) algorithm, ensuring maximum power extraction under varying environmental conditions. Wind energy is harvested using an AC-to-DC rectifier with an MPPT technique, optimizing power conversion from the variable wind resource. Battery charging and discharging operations are controlled through a bidirectional DC-DC buck-boost converter, enabling flexible energy storage management and smooth power flow between sources and loads. The magnetically linked power converter plays a crucial role in this system due to its inherent advantages, such as flexible control, high efficiency in power transmission, and galvanic isolation. The system's design ensures

soft-switching capability, high-density power transmission, and galvanic isolation, enabling efficient power management, reliable load sharing, and improved overall system performance under fluctuating renewable generation and load conditions.

1. INTRODUCTION

The widespread adoption of electric vehicles (EVs) plays a crucial role in the global transition to sustainable transportation and energy systems. Governments and industries are investing in EV infrastructure to reduce carbon emissions and mitigate climate change [1], [2]. However, large scale EV deployment places significant demands on power grids, especially regarding peak load management, power quality, and integration of distributed energy resources [3]. Therefore, designing efficient, reliable EV charging systems integrating renewable energy sources (RES) and energy storage is essential to meet rising electricity demand while maintaining grid stability [4]. Solar photovoltaic (PV) and wind power are widely accepted renewable for EV charging stations, offering environmentally friendly alternatives that reduce fossil fuel dependence and support decentralized generation [6], [5]. Yet, the intermittent and unpredictable nature of solar irradiance and wind speed challenges continuous and stable power supply [6]. Fluctuations in renewable power can cause voltage instability, degrade power quality, and increase grid stress if unmanaged [7]. Energy storage systems, particularly batteries, mitigate renewables' intermittency by storing excess energy during high generation and supplying it during peak demand or low production periods [8]. Coordinating multiple sources and loads including the grid, renewable, and storage requires sophisticated real-time power management and control strategies that ensure smooth power flow, optimal utilization, and stability under varying conditions [9],[10]. A key technology enabling such integration is the magnetically linked power converter, providing galvanic isolation via magnetic coupling, which enhances safety and reduces noise interference [11]. These converters facilitate flexible, bidirectional power flow, vital for energy exchange between AC and DC loads, such as EV chargers interfacing with multiple power sources [12]. Their soft-switching capability reduces switching losses and electromagnetic interference, improving efficiency and reliability [13], [14]. In the proposed system, the solar PV array connects to a DC-DC boost converter controlled by the Incremental Conductance (INC) Maximum Power Point Tracking (MPPT) algorithm, known for its high accuracy and fast response under varying irradiance and temperature [15]. Wind energy conversion uses an AC-to-DC rectifier with a dedicated MPPT algorithm optimized for variable-speed wind turbines to address wind variability [16], [17]. Battery management is achieved through a bidirectional DC-DC buck-boost converter, enabling flexible charging and discharging essential for energy balance and grid stability during fluctuating renewable output and load demand [18]. This converter also supports ancillary grid services like peak shaving and frequency regulation [19]. The architecture includes AC-DC load balancing enabled by the magnetically linked converter, dynamically distributing power between AC loads (e.g., household appliances, grid interface) and DC loads (mainly EV batteries), optimizing power flow and mitigating power quality issues such as harmonic distortion and voltage fluctuations [20]. The grid-connected configuration allows backup power and energy export; excess renewable energy can feed back into the grid, enhancing overall efficiency and enabling grid support, while the grid supplies power during deficits to ensure uninterrupted EV charging [21]. This bidirectional interaction requires advanced control strategies to synchronize power flow, maintain voltage stability, and comply with grid codes [22]. Advanced control algorithms manage the interactions between multiple energy sources, converters, and loads, ensuring smooth bidirectional power routing, decoupling control loops, and robust voltage/current regulation under diverse conditions. These controls are vital for resilience against faults, disturbances, and load changes, ensuring safe, efficient operation [23], [24]. Integrating magnetically linked converters with grid-connected solar PV, wind power, and battery storage offers a promising approach for advanced EV charging systems. This solution addresses renewable variability, load balancing, and power quality management, facilitating sustainable, reliable, and intelligent EV charging infrastructures [25]. The system's flexible, efficient power management enhances EV charging performance and supports smart grid and environmental sustainability goals.

2. System Configuration

The system configuration consists of a solar photovoltaic (PV) array connected to a DC-DC boost converter controlled by an Incremental Conductance (INC) MPPT algorithm, which ensures maximum power extraction by adapting to changing sunlight conditions. Wind energy is harnessed through a variable-speed wind turbine whose output AC power is converted to DC by an AC-DC rectifier with its own MPPT control to optimize energy capture from variable wind speeds. Both renewable sources feed into a common DC bus that supplies power to the loads and charges a battery storage system via a bidirectional DC-DC buck-boost converter. This converter manages charging and discharging of the battery, allowing energy storage during surplus generation and supply during high demand or low renewable availability. A magnetically linked power converter provides galvanic isolation and enables bidirectional power flow between AC and DC loads, balancing power distribution efficiently. The system is grid-connected to allow excess renewable energy to be fed back to the grid or draw power when renewable generation and battery storage are insufficient. Advanced control algorithms coordinate power flow, regulate voltages and currents, and ensure stability and reliable operation under varying load and generation conditions, making the system well-suited for sustainable and intelligent EV charging applications.

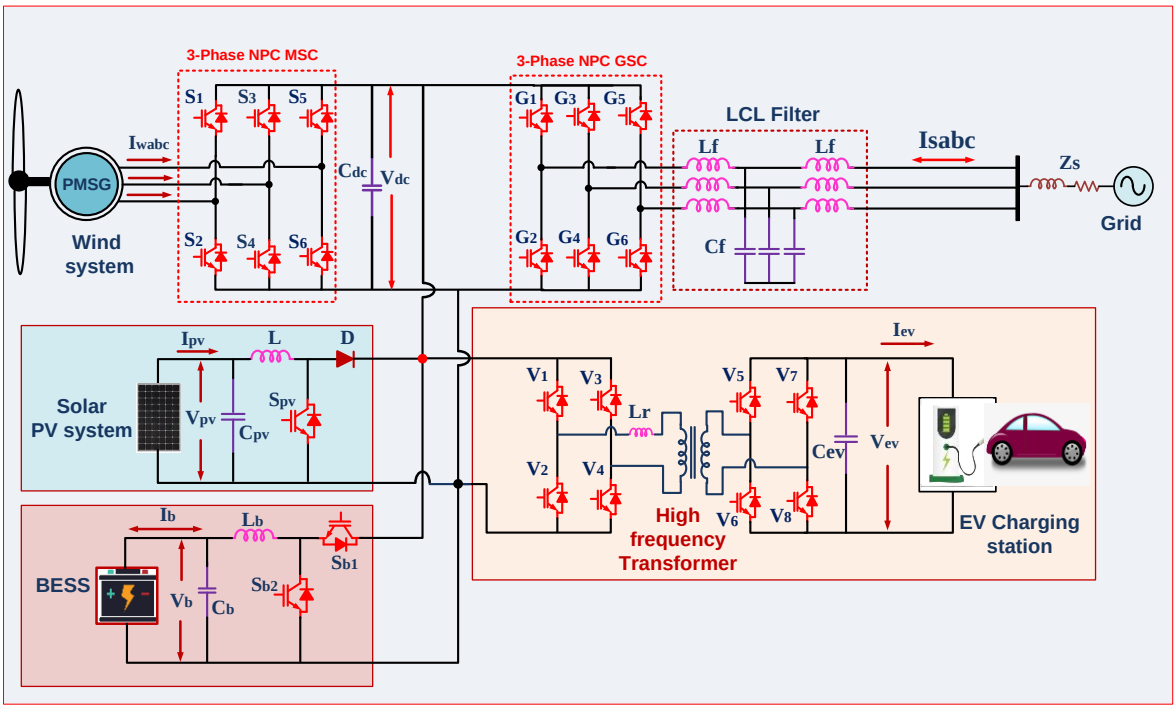

Fig.1 System topology for the smart grid connected to the EV charging station through DMLC

3. Mathematical Description of the Proposed Microgrid System

The proposed grid connected electric vehicle (EV) charging infrastructure integrates multiple energy sources including solar photovoltaic (PV) and wind energy, along with an energy storage system (ESS) and a bidirectional grid interface. These components are interconnected through magnetically linked power converters, which provide galvanic isolation, high frequency energy transfer, and modular scalability. The objective of this configuration is to ensure uninterrupted power supply for EV charging, support grid stability, enable Vehicle to Grid (V2G) operations, and optimize the utilization of renewable resources through advanced control techniques such as Maximum Power Point Tracking (MPPT), dq axis control, and fuzzy logic based energy management.

A. Solar Conversion System (SCS):

The Solar Conversion System (SCS) is crucial in current renewable energy systems, especially standalone and grid-connected microgrids that use solar photovoltaic (PV) electricity. The arrangement generally includes a PV panel array linked to a DC-link via a DC-DC boost converter, which regulates voltage and current for energy storage, load feeding, or grid injection. This converter raises the voltage to match the DC-link and maximizes PV module energy extraction using MPPT algorithms. The complete system must be precisely

modeled for high efficiency, stability, and dependability under dynamic environmental and load circumstances. Electrical behavior of the PV panel, boost converter, and energy management algorithms regulate the solar conversion system dynamic model. The PV module's DC voltage Vpv and current Ipv depend on solar irradiation and ambient temperature. The boost converter has an input inductor Lpv, input capacitor Cpv, duty cycle-controlled switching device U2, and DC-link-connected output capacitor Cdc. The differential equations below provide the system's state-space representation based on Kirchhoff's voltage and current laws:

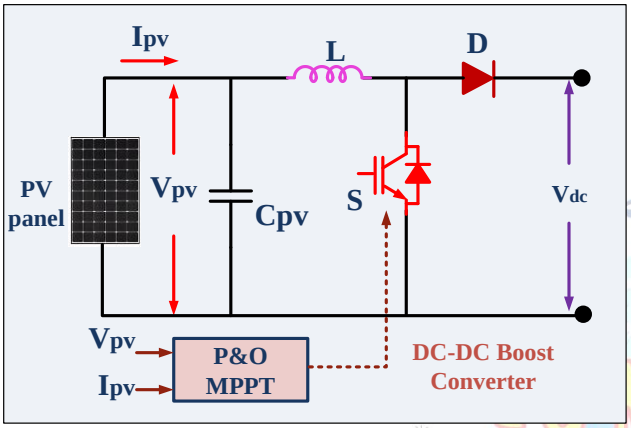

FIGURE 4. Solar energy system with controller.

$$\frac{dV_{pv}}{dt} = \frac{1}{C_{pv}}\left(D \cdot I_{pv} - I_{L_{pv}}\right) - \frac{V_{pv}}{L_{pv}} \quad (1)$$

$$\frac{dI_{pv}}{dt} = \frac{1}{L_{pv}}[C(1-U_2)V_{dC} - D_3] \quad (2)$$

$$\frac{dV_{dc}}{dt} = \frac{1}{C_{dc}}\left[D(1-U_2)I_{L_{pv}} - I_{O_{pv}}\right] + C \cdot D_4 \quad (3)$$

ILpv is the inductor current, IOpv is the PV stage current output into the load or battery storage, U2 is the MPPT controller control signal, and D3, D4 represent dynamic uncertainties in system parameters like parasitic inductance, switching losses, and sensor inaccuracies. The aforementioned model allows accurate control and simulation of solar energy harvesting under different circumstances. When the energy storage device, such as a battery bank or supercapacitor module, has capacity, the MPPT control technique is engaged to maximize PV array power. To keep PV panels at their maximum power point, MPPT algorithms like P&O, INC, and PI controller dynamically change duty cycle U2. The MPPT requirement is mathematical:

$$\frac{dP_{pv}}{dV_{pv}} = 0 \text{ at } MPP, \text{ where } P_{pv} = V_{pv} \cdot I_{pv} \quad (4)$$

MPPT mode is used in normal operation, and the control loop adjusts U2 to follow the PV module's peak power output. The system must avoid overcharging or DC overvoltage when the battery is completely charged, load demand is lower than PV production, and grid export is not allowed. In such instances, the SCS enters off-MPPT mode, where power optimisation is replaced by power flow balance and system integrity. A reference voltage Vref is computed in off-MPPT mode to decrease PV module power usage. This is critical for islanded systems when energy cannot be exported and excessive generation will destabilize the system. The equation for reference voltage is:

$$V_{ref} = \frac{P_L - P_{pv}}{I_{pv}} \quad (5)$$

where PL is the load power demand, and Ppv is the instantaneous PV output power. This reference is used in a voltage-mode control loop to modify the duty cycle and reduce the converter's input power draw, effectively curtailing PV generation to match the load.

From a design standpoint, the selection of boost converter components like Lpv and Cpv is critical for maintaining converter efficiency and reducing output ripple. The inductance is typically designed based on desired current ripple (ΔIL) and switching frequency fs:

$$L_{pv} = \frac{V_{pv} \cdot (1-D)}{f_s \cdot \Delta I_L} \quad (6)$$

Similarly, the input capacitance is sized to ensure voltage stability and reduce ripple across the PV terminals:

$$C_{pv} = \frac{I_{pv} \cdot D}{\Delta V_{pv} \cdot f_s} \quad (7)$$

Where ΔVpv is the acceptable voltage ripple (typically 1–2% of Vpv), and D is the converter duty cycle.

The DC-link output capacitor Cdc stabilizes downstream load or inverter stage voltage. Most calculations use output current ripple and DC voltage requirements. SCS is intended to function dependably in dynamic situations, adapt to changing irradiance and load circumstances, and work well with energy storage, inverters, and grid connections. In real-time applications, uncertainty treatment in system equations enhances resilience. Based on battery state-of-charge (SOC), load demand, and grid connection, advanced energy management algorithms dynamically transition between MPPT and off-MPPT.

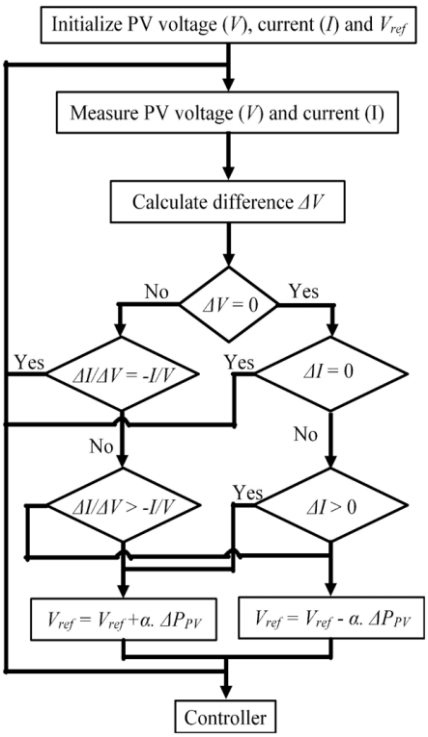

Fig 5. MPPT algorithm of the solar energy system

B. Configuration Wind Conversion System

1. Wind Turbine Modeling

The mathematical model of the wind power that can be transformed by the turbine:

Where:

- ϱ: Air density (kg/m³)
- A: Swept area of the blades = πR^2
- V_w: Wind speed (m/s)
- c_p: Power coefficient (function of tip speed ratio λ and pitch angle β)

$$\lambda = \frac{\omega_t R}{v_\omega} \quad (8)$$

Where:

- ωt: Turbine angular speed (rad/s)
- R: Radius of turbine blades (m)

The mechanical torque from the turbine:

$$T_m = \frac{P_{wind}}{\omega_t} \quad (9)$$

2. Permanent Magnet Synchronous Generator (PMSG) Modeling

The PMSG is modeled in the rotating dq-reference frame:

$$v_d = R_s i_d + L_d \frac{di_d}{dt} - \omega_e L_q i_q \quad (10)$$

$$v_q = R_s i_q + L_q \frac{di_q}{dt} + \omega_e (L_d i_d + \lambda_m) \quad (11)$$

$$T_e = \frac{3}{2} p\left[\lambda_m i_q + (L_d - L_q) i_d i_q\right] \quad (12)$$

Where:

- vd,vq: d- and q-axis voltages
- id,iq: d- and q-axis currents
- Rs: Stator resistance
- Ld,Lq: Inductances in d- and q-axis
- ωe: Electrical angular speed
- λm: Permanent magnet flux linkage
- TTe: Electromagnetic torque
- p: Number of pole pairs

For surface-mounted PMSGs, Ld=Lq, and torque simplifies to:

$$T_e = \frac{3}{2} p \lambda_m i_q \quad (13)$$

3. Active AC-DC Converter Modeling (VSC Rectifier)

The VSC rectifier operates as an active converter to regulate the DC-link voltage and control power flow. It converts the PMSG output AC to regulated DC.

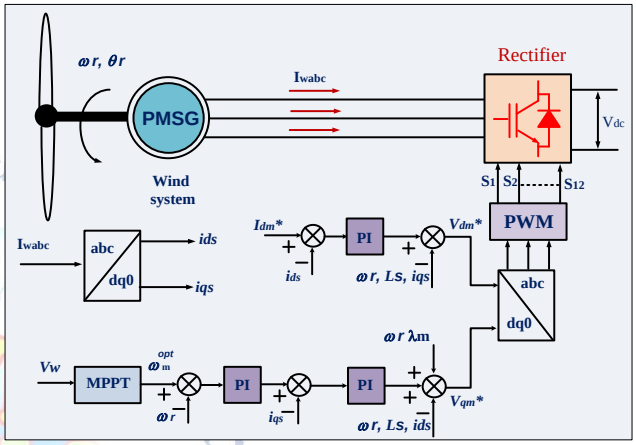

Fig.5 Wind conversion controller

a. Converter equations (abc to dq):

$$\frac{di_d}{dt} = \frac{1}{L}\left(v_d - Ri_d + \omega L i_q\right) \quad (14)$$

$$\frac{di_q}{dt} = \frac{1}{L}\left(v_q - Ri_q - \omega L i_d - \omega \lambda_m\right) \quad (15)$$

Where:

- vd,vq: Control voltages applied by the VSC
- L: Filter inductance
- R: Filter resistance

4. dq0 Current Controller Design

The dq0 controller maintains the reference values of *id∗ and iq∗:

- id∗=0: To avoid flux weakening and minimize losses
- iq∗: Controlled to regulate torque/power

Control loops:

- Inner loop: Regulates current using PI controllers
- Outer loop: MPPT regulates reference speed or power

$$v_d^* = Ri_d + L\frac{di_d}{dt} - \omega L i_q - K_{pd}(i_d^* - i_d) + K_{id}\int (i_d^* - i_d)\, dt \quad (16)$$

$$v_q^* = Ri_q + L\frac{di_q}{dt} - \omega L i_q - K_{pq}(i_q^* - i_q) + K_{iq}\int (i_q^* - i_q)\, dt$$

(17)

5. MPPT Control Strategy

a. Tip Speed Ratio (TSR) Method:

Keep λ at optimal value λopt for maximum Cp:

$$\omega_t^* = \frac{\lambda_{opt} v_\omega}{R} \qquad (18)$$

Use speed controller (PI) to generate torque reference:

$$T_e^* = K_p(\omega_t^* - \omega_t) + K_i\int (\omega_t^* - \omega_t)\, dt \qquad (19)$$

From torque, derive iq∗ using:

$$i_q^* = \frac{2T_e^*}{3p\lambda_m} \qquad (20)$$

b. Power Signal Feedback (PSF):

Estimate $P_{opt} = k\omega_t^3$ and use outer-loop PI controller to track it.

C. Bidirectional DC-DC Buck-Boost Battery Converter Configuration

The bidirectional DC-DC buck-boost converter is a versatile power electronic device designed to control the flow of energy between a battery and the DC bus. It allows energy to flow in two directions:

- From the DC bus to the battery for charging (buck mode), and
- From the battery to the DC bus for discharging (boost mode).

This bidirectional operation is crucial in renewable energy systems and EV charging infrastructures for efficient energy storage management and grid support functionalities such as peak shaving, load leveling, and backup power supply.

- In buck mode (charging), the converter steps down the DC bus voltage to a lower voltage suitable for charging the battery. The energy flows from the DC bus to the battery, and the switch duty cycle D controls the average voltage and current supplied to the battery.
- In boost mode (discharging), the converter steps up the battery voltage to match or exceed the DC bus voltage, allowing the battery to supply power back to the DC bus or grid.

The control strategy adjusts the duty cycle D dynamically based on battery State of Charge (SOC), load demand, and grid conditions.

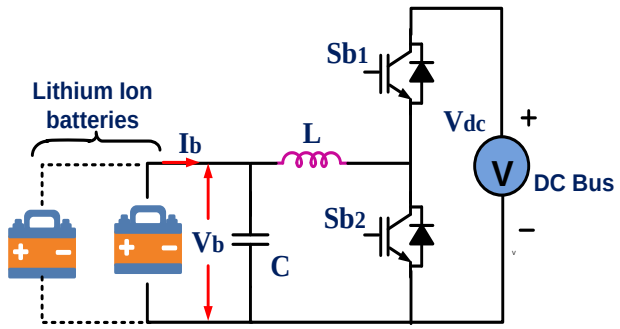

Fig.6 principle operation bidirectional dc-dc buck boost converter

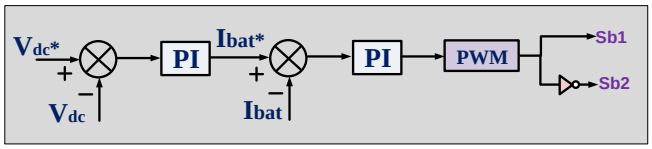

Fig. 7 double loop ev charging controller

1. Mathematical Modeling and Key Formulas

a. Buck Mode (Charging)

When the switch is **ON** (for a fraction DDD of the switching period TTT), the inductor current increases, storing energy:

$$V_{dc} - V_L - V_{bat} = 0 \qquad (21)$$

which simplifies to:

$$V_L = V_{dc} - V_{bat} \qquad (22)$$

The inductor current slope during ON-time:

$$\frac{dI_L}{dt} = \frac{V_{dc} - V_{bat}}{L} \qquad (23)$$

When the switch is OFF (for D1−D of T), the inductor releases energy to the battery:

$$V_L = -V_{bat} \qquad (24)$$

with the inductor current slope:

$$\frac{dI_L}{dt} = -\frac{V_{bat}}{L} \qquad (25)$$

The average voltage across the inductor over one switching period must be zero in steady-state:

$$(V_{dc} - V_{bat}) + (1 - D)(-V_{bat}) = 0 \qquad (26)$$

Solving for battery voltage:

$$V_{bat} = DV_{dc} \qquad (27)$$

This shows the battery voltage is a fraction of the DC bus voltage proportional to the duty cycle DDD in buck mode.

b. Boost Mode (Discharging)

In boost mode, the battery voltage is boosted to the DC bus voltage. When the switch is **ON**, the inductor is charged from the battery:

$$V_L = V_{bat} \quad (28)$$

and

$$\frac{dI_L}{dt} = \frac{V_{bat}}{L} \quad (29)$$

When the switch is OFF, the inductor current flows through the diode into the DC bus:

$$V_L = V_{dc} - V_{bat} \quad (30)$$

With

$$\frac{dI_L}{dt} = \frac{V_{dc} - V_{bat}}{L} \quad (31)$$

The steady-state condition (average inductor voltage zero):

$$DV_{bat} + (1 - D)(V_{dc} - V_{bat}) = 0 \quad (32)$$

Solving for Vdc:

$$V_{dc} = \frac{V_{bat}}{1-D} \quad (33)$$

This indicates the DC bus voltage is a multiple of battery voltage depending on the duty cycle in boost mode.

4. Configuration of Bidirectional DC-DC Dual Active Bridge (DAB) Converter

The Dual Active Bridge (DAB) Converter is a high-frequency isolated bidirectional power converter consisting of:

1. Two full-bridge converters:
   - One on the primary side (connected to source/load like a DC grid or PV).
   - One on the secondary side (connected to battery/ESS).
2. High-frequency transformer:
   - Provides galvanic isolation.
   - Enables voltage scaling between input and output.
3. High-frequency switching devices (MOSFETs/IGBTs) in each full bridge.
4. DC capacitors on both input and output sides for voltage smoothing.

The DAB converter works by applying phase-shifted square wave voltages from the two active bridges to the transformer. Power transfer between the two sides is regulated by adjusting the phase shift (φ) between the primary and secondary voltages.

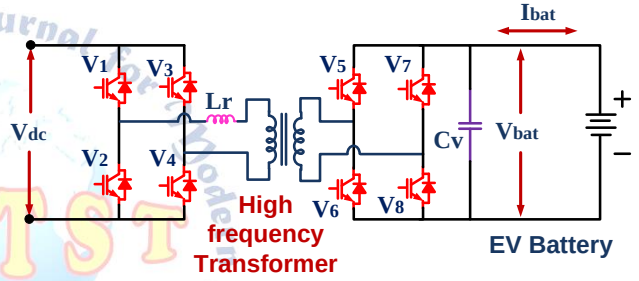

Fig.8 dual active bridge converter for fast electric vehicle charging station

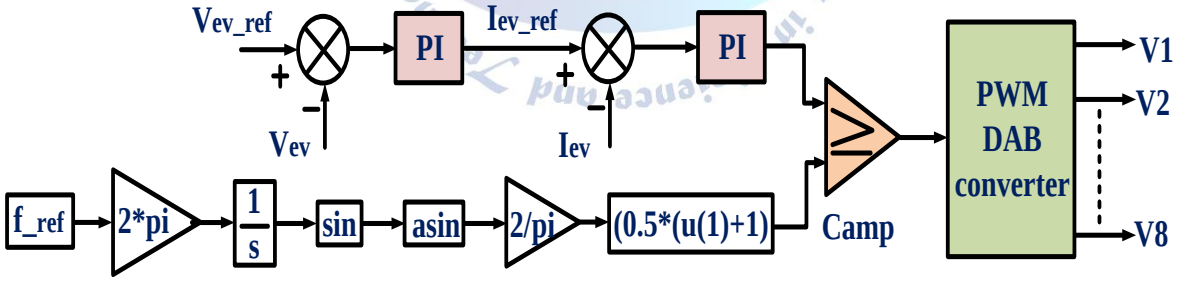

Fig.9 controller design for dual active bridge converter for fast electric vehicle charging station

1. Power Flow from Primary to Secondary (Charging Mode):
   - Occurs when the primary voltage leads the secondary voltage (positive phase shift).
   - Energy flows from DC source/grid to battery.
2. Power Flow from Secondary to Primary (Discharging Mode):
   - Occurs when the secondary voltage leads the primary voltage (negative phase shift).
   - Energy flows from battery to DC grid or loads.

This phase-shift control enables bidirectional power transfer with high efficiency, fast response, and soft-switching (ZVS).

a. Power Transfer Equation:

The average power transferred from primary to secondary is:

$$P = \frac{nV_1V_2}{\omega L} \cdot \phi \cdot \left(1 - \frac{|\phi|}{\pi}\right) \text{ (for small } \phi) \quad (34)$$

Where:

- ω=2πfs

- $\phi \in [-\pi, \pi]$

In simplified and commonly used linearized form (for small φ):

$$P = \frac{nV_1V_2}{\omega L} \cdot \phi \quad (35)$$

This equation shows that the power transferred is:

- Proportional to the phase shift φ
- Bidirectional depending on the sign of φ
- Scalable with voltage and frequency

5. Grid-Side Converter Control Using PI Controller

The grid-side converter (GSC) in a direct current (DC) microgrid is in charge of regulating the DC voltage and power factor (PFC) as well as the two-way flow of power from the grid to the DC bus. One popular and effective power conversion tool is the bidirectional AC-DC voltage source converter, often known as the neutral-point clamped (NPC) VSC. The grid-side converter's control strategy is put into action in the synchronous dq reference frame, where the reactive power is controlled by the q-axis and the DC-link voltage is controlled by the d-axis. To maintain steady and effective functioning, a PI controller is used to regulate Vd, Vq, Id, and Iq. Two parts make up the control structure: one that regulates the DC-link voltage and another that controls the grid currents. From the voltage controller, we calculate the reference dq currents (Idref and Iqref), and to reduce the error between the reference and real values, we use a PI controller. By regulating the DC-link voltage, the d-axis control keeps the active power flow under control, and by minimizing or controlling the reactive power, the q-axis control does the same. The Park transformation of the three-phase AC system is used to determine the current and voltage equations for the grid-side converter, which allows for more efficient regulation of the power flow.

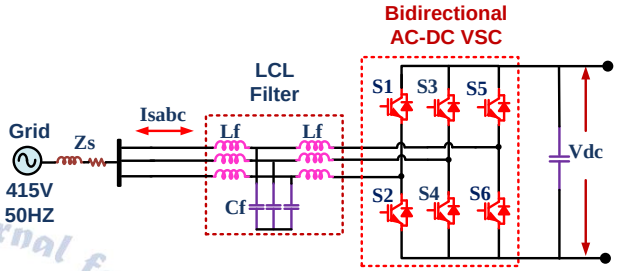

Fig.6 designing of bidirectional AC–DC voltage source converter

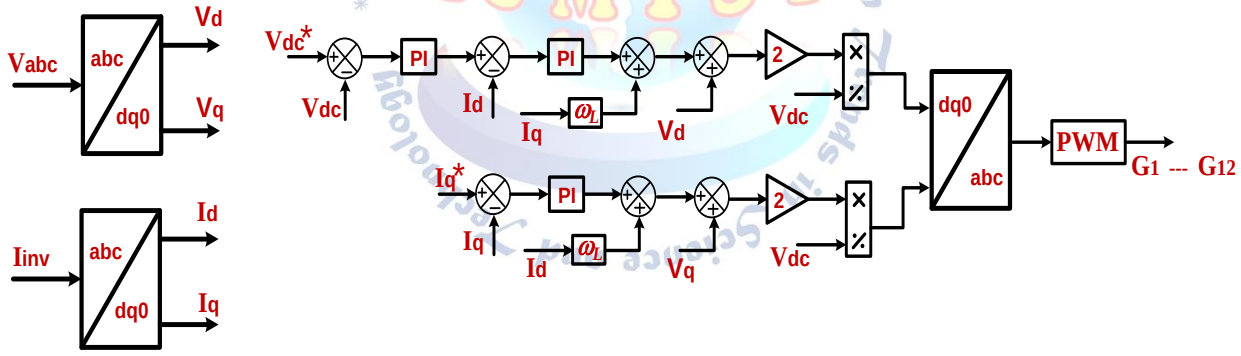

Fig. 10 Grid conversion controller

1. d-q Axis Voltage Equations

$$V_d = R_S I_d + L_s \frac{dI_d}{dt} - \omega L_s Iq + V_{gd} \quad (36)$$

$$V_q = R_S I_q + L_s \frac{dI_q}{dt} + \omega L_s I_d + V_{gq} \quad (37)$$

3. Active and Reactive Power Equations

$$P = \frac{3}{2}\left(V_d I_d + V_q I_q\right) \quad (38)$$

$$Q = \frac{3}{2}\left(V_q I_d - V_d I_q\right) \quad (39)$$

Where: P = Active power (W), Q = Reactive power (VAR)

4. PI Controller for d-q Current Control

$$V_d^{ref} = K_p\left(I_d^{ref} - I_d\right) + K_i \int \left(I_d^{ref} - I_d\right) dt \quad (40)$$

$$V_q^{ref} = K_p\left(I_q^{ref} - I_q\right) + K_i \int \left(I_q^{ref} - I_q\right) dt \quad (41)$$

Where: Kp,Ki = PI controller gains, Vdref,Vqref = Reference d-q axis voltages

The PI controller ensures accurate current regulation by adjusting the error between reference and actual d-q currents. The grid-side converter uses these control strategies to maintain power quality, regulate the DC-link voltage, and manage bidirectional power flow between the grid and the DC microgrid efficiently.

5. PI Controller for DC-Link Voltage Regulation

The DC-link voltage PI controller generates the reference d-axis current:

$$I_d^{ref} = K_{P_{dc}}\left(V_{dC}^{ref} - V_{dc}\right) + K_{I_{dc}} \int \left(V_{dC}^{ref} - V_{dc}\right) dt \quad (42)$$

Where: Idref = Reference d-axis current (A), Vdcref = Reference DC-link voltage (V), Vdc = Actual DC-link voltage (V), Kpdc,Kidc = PI controller gains for DC voltage regulation

This control strategy ensures that the DC-link voltage remains stable under varying grid conditions, enabling efficient energy exchange between the grid and the DC microgrid.

6. Simulation Results and Discussion

A. Working and Operational Behavior of the Proposed Grid-Connected EV Charging System

The proposed system operates by integrating solar photovoltaic, wind energy, and a battery energy storage system to power both AC and DC loads, including electric vehicle charging. These sources are managed through a grid-connected configuration using magnetically linked converters. A dq0 current controller and DC-link voltage regulation technique ensure stable power delivery under changing conditions. At the start of operation, when solar irradiance and wind speeds are high, the power generated from renewable sources is sufficient to meet the load demand. During this time, the grid and battery storage remain inactive as there is no need for additional power support. As environmental conditions change, such as a decrease in sunlight or wind speed, the power output from the renewable sources reduces. This causes an energy imbalance where the demand exceeds the supply. To compensate, the grid provides the required additional power to maintain uninterrupted operation. When the renewable energy is temporarily underutilized or the load is lower, the battery energy storage system begins to charge from the grid. Conversely, when the system detects an increased load demand or further reduction in renewable generation, the battery discharges its stored energy to support the load and reduce dependency on the grid. When electric vehicles begin charging, they draw power from both the grid and the battery storage depending on availability. The system intelligently manages the charging process, coordinating the flow of power among sources to maintain a constant DC-link voltage. The dq0 control method helps to maintain grid current quality and system stability during these transitions. The system effectively balances renewable generation, grid power, and energy storage to ensure reliable electric vehicle charging and load management in all operating conditions.

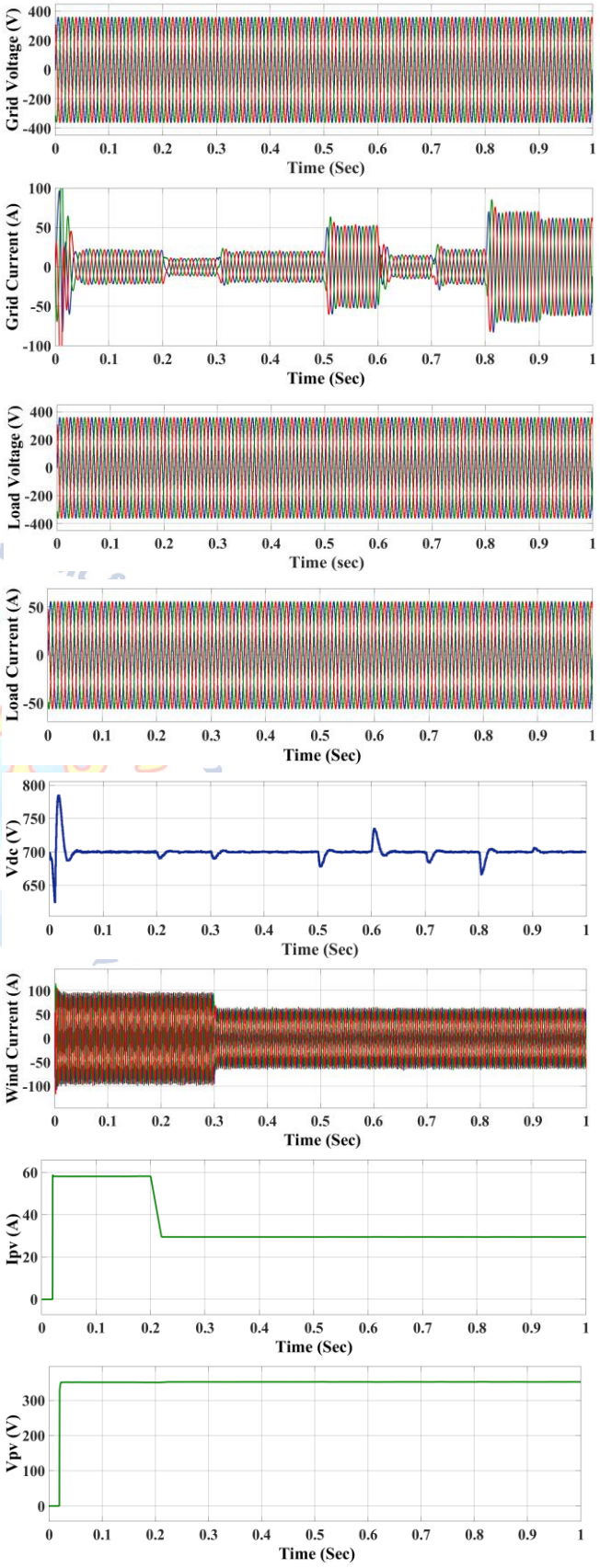

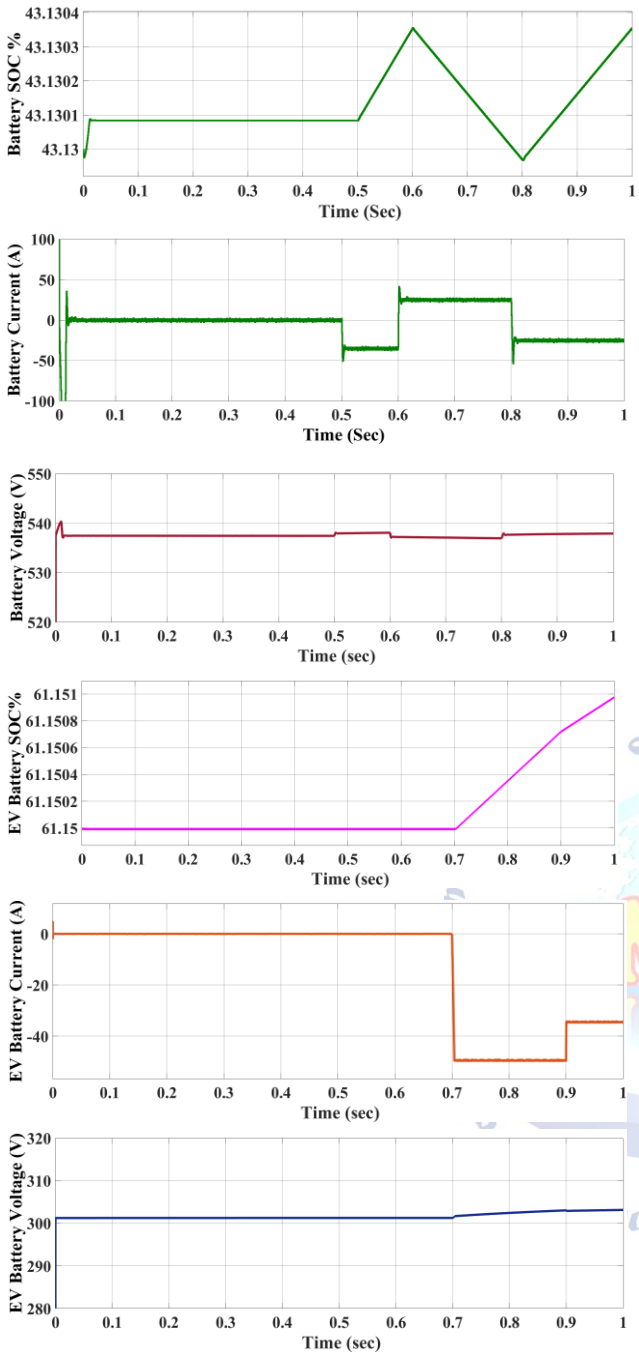

Fig.7 Simulation results of Grid-Connected Solar, Wind, and BESS for EV Charging System

B. Dynamic Operational Response of the Grid-Connected Solar, Wind, BESS for EV Charging System

The proposed grid-connected electric vehicle (EV) charging system, integrating 20 kW solar photovoltaic (PV), 20 kW wind generation, and a 50 kW battery energy storage system (BESS), was simulated for a total run time of 1 second using MATLAB/Simulink. The system is designed to manage dynamic energy flow among renewable sources, energy storage, electric vehicles, and grid support through a dq0-based grid current and DC-link voltage control strategy, ensuring power balance and system stability under varying conditions. During the initial period from 0 to 0.2 seconds, the solar PV system operates under ideal irradiance conditions of 1000 W/m², producing its full capacity of 20 kW. This energy is supplied directly to meet part of the total load, which includes a 30 kW AC load and a 10.8 kW EV charging demand. The wind system also generates 20 kW at a wind speed of 12 m/s, enabling full renewable penetration without requiring support from the grid or battery systems during this interval. From 0.2 to 0.3 seconds, the solar irradiance drops from 1000 W/m² to 500 W/m², reducing the solar output accordingly. Simultaneously, at 0.3 seconds, the wind speed decreases from 12 m/s to 10 m/s, resulting in a reduction of wind power generation from 20 kW to 10 kW. These combined reductions in renewable generation lead to a power deficit. During this period, the grid dynamically compensates for the shortfall, ensuring continuous power delivery and load balancing. The BESS and EV battery remain idle and are neither charging nor discharging in this time frame. From 0.5 to 0.6 seconds, the BESS begins to charge from the grid at a power level of 20 kW due to available surplus from the grid and reduced load demand. This charging process is governed by the bidirectional DC-DC converter, efficiently regulating the charge flow. Subsequently, from 0.6 to 0.8 seconds, the BESS transitions to discharge mode, supplying power back to the DC link and reducing the reliance on grid power while stabilizing the overall load demand. At 0.7 seconds, the EV battery begins charging with a demand of 18 kW. This charging power is sourced jointly from the discharging BESS and the utility grid, demonstrating the flexible coordination of storage and grid support to fulfill critical charging needs. Finally, during the interval from 0.8 to 1 second, the BESS resumes charging at 18 kW, drawing power from the grid while the solar and wind sources each contribute 10 kW, maintaining system continuity and optimizing renewable utilization. The dq0 control strategy ensures that the grid current remains sinusoidal with low harmonic distortion throughout all scenarios, while the DC-link voltage is tightly regulated within permissible limits. These results confirm the system's ability to respond adaptively to renewable fluctuations, maintain stable operation, and provide reliable EV charging with optimal energy source coordination.

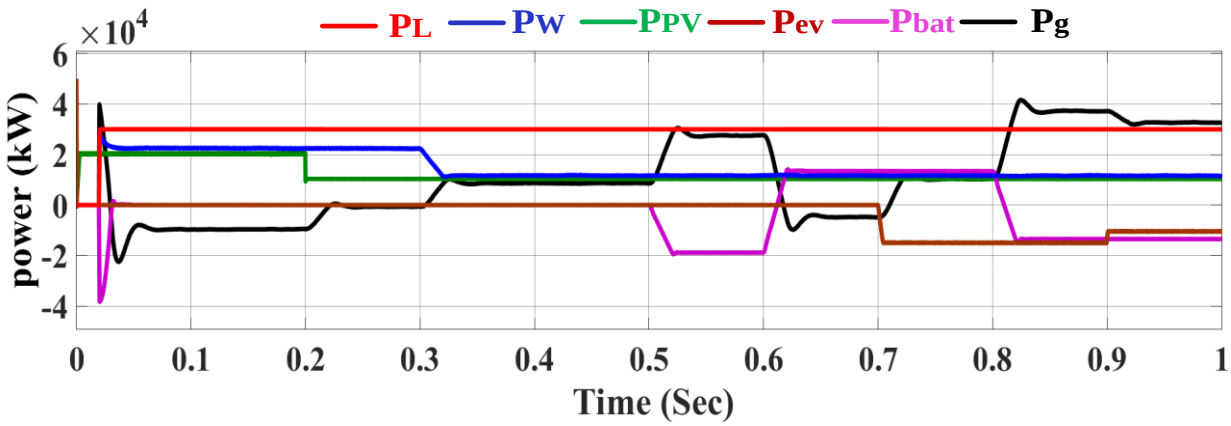

Fig.15 Simulation Analysis and Dynamic Operational Response of the Grid-Connected EV Charging System

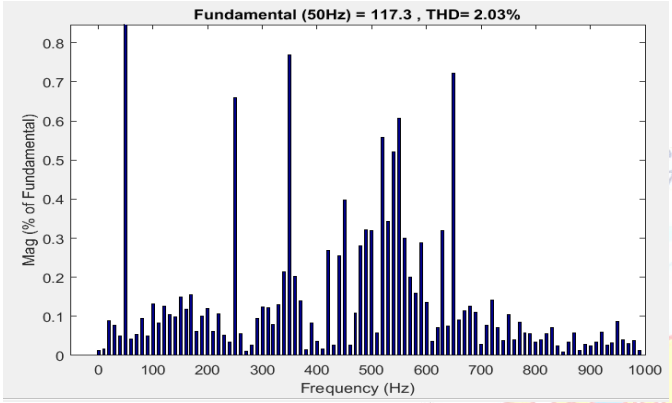

Fig. 16 Grid current THD value

7. Conclusion

This study presents a robust and integrated solution for electric vehicle charging by utilizing advanced power management techniques combined with magnetically linked power converters and multiple renewable energy sources. The proposed system successfully incorporates solar photovoltaic, wind energy, and battery storage to form a unified energy infrastructure that is capable of managing both AC and DC loads efficiently. The use of Incremental Conductance MPPT for solar panels and an optimized MPPT technique for wind ensures that maximum power is consistently extracted from renewable sources despite fluctuating environmental conditions. The bidirectional DC-DC buck-boost converter enables seamless battery operation, supporting energy storage during excess generation and discharging during high demand. The inclusion of a magnetically linked power converter enhances system performance through galvanic isolation, soft-switching operation, and high-efficiency energy transfer. Altogether, the system demonstrates superior flexibility, improved power quality, and increased reliability for EV charging stations. It supports sustainable energy utilization and strengthens the connection between electric mobility and renewable integration, paving the way for a smarter and greener energy future.

Conflict of interest statement

Authors declare that they do not have any conflict of interest.

REFERENCES

[1] Liserre, M.; Sauter, T.; Hung, J.Y., "Future Energy Systems: Integrating Renewable Energy Sources into the Smart Power Grid Through Industrial Electronics," Industrial Electronics Magazine, IEEE , vol.4, no.1, pp.18,37, March 2010.

[2] Bose, B.K., "Global Energy Scenario and Impact of Power Electronics in 21st Century," Industrial Electronics, IEEE Transactions on , vol.60, no.7, pp.2638,2651, July 2013.

[3] Blaabjerg, F.; Zhe Chen; Kjaer, S.B., "Power electronics as efficient interface in dispersed power generation systems," Power Electronics, IEEE Transactions on , vol.19, no.5, pp.1184,1194, Sept. 2004.

[4] Jamehbozorg, A.; Radman, G., "Small Signal Analysis of Power Systems With Wind and Energy Storage Units," Power Systems, IEEE Transactions on , vol.30, no.1, pp.298,305, Jan. 2015.

[5] Vargas, L.S.; Bustos-Turu, G.; Larrain, F., "Wind Power Curtailment and Energy Storage in Transmission Congestion Management Considering Power Plants Ramp Rates," Power Systems, IEEE Transactions on , vol.PP, no.99, pp.1,9, 2015.

[6] Quanyuan Jiang; Yuzhong Gong; Haijiao Wang, "A Battery Energy Storage System Dual-Layer Control Strategy for Mitigating Wind Farm Fluctuations," Power Systems, IEEE Transactions on , vol.28, no.3, pp.3263,3273, Aug. 2013.

[7] Derakhshandeh, S.Y.; Masoum, A.S.; Deilami, S.; Masoum, M.A.S.; Hamedani Golshan, M.E., "Coordination of Generation Scheduling with PEVs Charging in Industrial Microgrids," Power Systems, IEEE Transactions on , vol.28, no.3, pp.3451,3461, Aug. 2013.

[8] Yilmaz, M.; Krein, P.T., "Review of Battery Charger Topologies, Charging Power Levels, and Infrastructure for Plug-In Electric and

Hybrid Vehicles," Power Electronics, IEEE Transactions on , vol.28, no.5, pp.2151,2169, May 2013.

[9] R. Sioshansi and P. Denholm, "Emissions Impacts and Benefits of Plug- In Hybrid Electric Vehicles and Vehicle-to-Grid Services," Environmental Science & Technology, vol. 43, no. 4, pp. 1199-204, Feb. 2009.

[10] C. Thomas, "Fuel Cell and Battery Electric Vehicles Compared," International Journal of Hydrogen Energy, p. 262512, 2009.

[11] M. Yilmaz and P. T. Krein, "Review of the Impact of Vehicle-to-Grid Technologies on Distribution Systems and Utility Interfaces," IEEE Transactions on Power Electronics, vol. 28, no. 12, pp. 5673-5689, Dec. 2013.

[12] Mischinger, S.; Hennings, W.; Strunz, K., "Integration of surplus wind energy by controlled charging of electric vehicles," Innovative Smart Grid Technologies (ISGT Europe), 2012 3rd IEEE PES International Conference and Exhibition on , vol., no., pp.1,7, 14-17 Oct. 2012.

[13] Kramer, B.; Chakraborty, S.; Kroposki, B., "A review of plug-in vehicles and vehicle-to-grid capability," Industrial Electronics, 2008. IECON 2008. 34th Annual Conference of IEEE , vol., no., pp.2278,2283, 10-13 Nov. 2008

[14] Kisacikoglu, M.C.; Ozpineci, B.; Tolbert, L.M.; Wang, F., "Singlephase inverter design for V2G reactive power compensation," Applied Power Electronics Conference and Exposition (APEC), 2011 Twenty- Sixth Annual IEEE , vol., no., pp.808,814, 6-11 March 2011.

[15] Da Qian Xu; Joos, G.; Levesque, M.; Maier, M., "Integrated V2G, G2V, and Renewable Energy Sources Coordination Over a Converged Fiber- Wireless Broadband Access Network," Smart Grid, IEEE Transactions on, vol.4, no.3, pp.1381,1390, Sept. 2013.

[16] Yilmaz, M.; Krein, P.T., "Review of the Impact of Vehicle-to-Grid Technologies on Distribution Systems and Utility Interfaces," Power Electronics, IEEE Transactions on , vol.28, no.12, pp.5673,5689, Dec. 2013.

[17] Mitra, P.; Venayagamoorthy, G.K., "Wide area control for improving stability of a power system with plug-in electric vehicles," Generation, Transmission & Distribution, IET , vol.4, no.10, pp.1151,1163, October 2010.

[18] Galus, Matthias D.; Waraich, R.A.; Noembrini, F.; Steurs, K.; Georges, G.; Boulouchos, K.; Axhausen, K.W.; Andersson, G., "Integrating Power Systems, Transport Systems and Vehicle Technology for Electric Mobility Impact Assessment and Efficient Control," Smart Grid, IEEE Transactions on , vol.3, no.2, pp.934,949, June 2012.

[19] [19] Molderink, A.; Bakker, V.; Bosman, M.G.C.; Hurink, J.L.; Smit, G.J.M., "Management and Control of Domestic Smart Grid Technology," Smart Grid, IEEE Transactions on , vol.1, no.2, pp.109,119, Sept. 2010.

[20] M. A. Rahman, M. R. Islam, K. M. Muttaqi, and D. Sutanto, ''A magnetic linked multiport fractional converter for application to variable speed wind power generating systems,'' IEEE J. Emerg. Sel. Topics Ind. Electron., vol. 3, no. 2, pp. 321–331, Apr. 2022.

[21] Y. Chen, P. Wang, Y. Elasser, and M. Chen, ''Multicell reconfigurable multi-input multi-output energy router architecture,'' IEEE Trans. Power Electron., vol. 35, no. 12, pp. 13210–13224, Dec. 2020.

[22] X.-F. He, Z. Zhang, Y.-Y. Cai, and Y.-F. Liu, ''A variable switching frequency hybrid control for ZVS dual active bridge converters to achieve high efficiency in wide load range,'' in Proc. IEEE Appl. Power Electron. Conf. Expo., Mar. 2014, pp. 1095–1099.

[23] Y. Guo, J. Meng, Y. Wang, and C. Wang, ''A virtual DC machine control strategy for dual active bridge DC–DC converter,'' in Proc. IEEE Innov. Smart Grid Technol., May 2019, pp. 2384–2388.

[24] Y. Guo,W. Ma, J. Meng, and Y.Wang, ''A virtual inertia control strategy for dual active bridge DC–DC converter,'' in Proc. 2nd IEEE Conf. Energy Internet Energy Syst. Integr. (EI), Oct. 2018, pp. 1–5.

[25] X. Gao, L. Fu, F. Ji, and Y. Wu, ''Virtual current based direct power control strategy of dual-active-bridge DC–DC converter,'' in Proc. IEEE Int. Conf. Mechatronics Autom. (ICMA), Aug. 2019, pp. 1947–1952.